EUROPEAN ORGANIZATION FOR NUCLEAR RESEARCH

July 20, 1997

Neutral Current Four-fermion Production in e^+e^- Interactions at 130 GeV $\leq \sqrt{s} \leq$ 172 GeV

The L3 Collaboration

Abstract

A study of neutral current four-fermion processes is performed, using the data collected by the L3 detector at LEP during the high energy runs at centre-of-mass energies 130-136, 161 and 170-172 GeV, where an integrated luminosity of 4.9, 10.7 and 10.1 pb^{-1} was respectively collected.
The $\ell\ell\ell'\ell'$ and $\ell\ell$qq (ℓ = e, μ or τ) final states are investigated. The total cross section for the processes $\ell\ell\ell'\ell'$ and $\ell\ell$qq is measured and found to be in agreement with the Standard Model prediction.

Submitted to *Int. Europhysics Conference on High Energy Physics, Jerusalem '97*

Introduction

Observation of four-fermion events above expectations from Standard Model would signal the existence of new physics, like for example, the production of the Standard Model Higgs boson [1].

The four-fermion final states arise from several production mechanisms, each giving a contribution to the cross section in a specific configuration of the final-particle phase space. In Fig. 1 all the possible classes of neutral current four-fermion production diagrams are shown. The largest total cross section is due to the *multiperipheral* diagrams. Here, two quasi-real photons are exchanged in the t-channel giving rise to forward electrons/positrons plus a fermion pair with a non-resonant structure (the so-called two-photon processes). These classes of processes do not contribute to final states interesting for the studies of Z production. In the latter case, if a $\mathrm{e^+e^-}$ pair is present in the final state, the main contributions come from the *bremsstrahlung* diagrams, otherwise the *conversion* contribute the most, mainly with an initial state radiative photon and a Z boson on its mass shell. This is in contrast with the situation at LEP1, where the *annihilation* mechanism dominates.

Important characteristics of the four-fermion events are the energy and angular distributions of the outgoing fermions. If a $\mathrm{e^+e^-}$ pair is present in the final state, due to the t-channel, the electrons tend to have the beam energy and to be emitted along the beam-direction. The other fermions in the event prefer lower energies but still are predominantly generated in the forward direction. If no $\mathrm{e^+e^-}$ pair is present in the final state, the fermions have a flat energy distribution up to the beam energy and a forward angular distribution.

In most of the cases a photon is present in the final state, for istance at $\sqrt{s} = 172$ GeV in $\sim$ 35 % of the cases there are only four fermions, in $\sim$ 50 % of the cases there is also a photon and in $\sim$ 15 % of the cases there are two photons; most of the photons go along the beam-pipe and they have an energy of few GeV.

This paper analyses final states produced by neutral gauge boson exchange, i.e. γ or Z; these final states were already observed at LEP1 [2]. They can be classified as follows: $\ell\ell$qq events and $\ell\ell\ell'\ell'$ events, where $\ell = \mathrm{e}$, μ or τ.

1 Data and Monte Carlo Samples

The data were collected by the L3 detector [3] at LEP in 1995 and 1996. The data sample used corresponds to 4.9 $\mathrm{pb^{-1}}$, 10.7 $\mathrm{pb^{-1}}$ and 10.1 $\mathrm{pb^{-1}}$ at $\sqrt{s} =$ 130.3-136.3 GeV, 161.3 GeV and 170.3-172.3 GeV respectively.

The EXCALIBUR [4] Monte Carlo was used to simulate the four-fermion events; these events were generated requiring a minimum momentum of the outgoing fermions of 1 GeV, a minimum invariant mass of each combination of two fermions of 1 GeV and at least 5^0 of the outgoing fermions with respect to the beam axis, in this way reducing the contribution from the *multiperipheral* diagrams.

Possible background comes from fermion pair production, charged current four-fermion events and two-photon physics, if at least one of the outgoing fermions has an angle with respect to the beam axis lower than 5^0. Concerning the fermion pair production, the radiative Bhabha events ($\mathrm{e^+e^-} \to \mathrm{Z}/\gamma^* \to \mathrm{e^+e^-}\gamma$) were generated using BHAGENE 3 [5]. The radiative di-muons ($\mathrm{e^+e^-} \to \mathrm{Z}/\gamma^* \to \mu^+\mu^-\gamma$) and the di-taus ($\mathrm{e^+e^-} \to \mathrm{Z}/\gamma^* \to \tau^+\tau^-(\gamma)$) samples were generated using KORALZ 4.02 [6]. The hadronic events ($\mathrm{e^+e^-} \to \mathrm{Z}/\gamma^* \to \mathrm{q\overline{q}}(\gamma)$) were generated with PYTHIA 5.72 [7]. Concerning the background coming from the charged current four-fermion processes, i.e. where the W boson takes part to the process, KORALW 1.21 [8] was used to simulate the $e^+e^- \to$ WW process, while PYTHIA 5.718 [7] was used to simulate the $e^+e^- \to$ Weν process. Finally the two-photon events were generated with PYTHIA 5.72 [7].

The L3 detector response is simulated using the GEANT 3.15 program [9], which takes into account the effects of energy loss, multiple scattering and showering in the detector. The GHEISHA program [10] was used to simulate hadronic interactions in the detector.

Four-fermion selection

In the following, the selection criteria for the lepton identification are explained, then the event selections are described. Two different event selections are developed for the low multiplicity and high multiplicity topologies. The first selection is dedicated to the $\ell\ell\ell'\ell'$ final states, while the second one is dedicated to the $\ell\ell$qq final states.

Lepton identification

Electrons

Electrons are identified as energy depositions in the electromagnetic calorimeter consistent with electromagnetic showers. If the calorimetric cluster is within $|\cos\theta| < 0.95$, a track is required to be associated to it.

The track must have a momentum greater than 0.5 GeV and a distance of closest approach to the interaction vertex less than 10 mm. The same requirements for a track are also used for the identification of the other leptons.

The cluster is selected requiring $E_\mathrm{B} > 1$ GeV, being E_B the energy in the e.m. calorimeter. The corresponding deposition in the hadron calorimeter has to be consistent with the tail of an electromagnetic shower (i.e. $E_\mathrm{H}/E_\mathrm{B} < 0.2$ and $E_\mathrm{H} < 5$ GeV, where E_H is the energy in the hadronic calorimeter). Finally the ratio of the energy in a 3x3 crystal matrix over the energy in a 5x5 crystal matrix around the center of gravity of the electromagnetic shower ($\Sigma 9/\Sigma 25$) is required to be greater than 0.93.

If the identified electrons are in a hadronic environment, as it happens for the $\ell\ell$qq final states, the quality cuts are tightened and isolation cuts are applied to reject the background coming from the semileptonic decays of the hadrons. Thus it is required $\chi^2_\mathrm{em} < 4.5$, where the χ^2_em is the estimator of the consistency of the shower with an electromagnetic one, and $\Sigma 9/\Sigma 25$ larger than 0.975. Moreover the difference in the ϕ angle between the electromagnetic cluster and the track in the central tracking chamber is asked to be less than 10 mrad and finally there must not be more than one track in a 20^0 half opening cone around the electron.

Muons

Muons are identified as tracks in the muon chambers pointing to the interaction point. The calorimetric clusters and the tracks in the central chambers matched within 100 mrad in ϕ and θ are associated to those muons.

The following isolation criteria are applied to the identified muons if they are in a hadronic environment: the calorimetric energy in the region between 5^0 and 10^0 half opening cone around the muon direction, excluding the muon energy, has to be less than 5 GeV. Moreover the number of TEC tracks in a 20^0 half opening cone around the muon direction has to be less than 2, and finally at most one calorimetric cluster is allowed in the region between 5^0 and 20^0 half opening cones.

Taus

The hadronically decaying taus are identified as one, two or three prongs with calorimetric energy greater than 2 GeV. Two prong taus are kept to take into account a possible TEC inefficiency. The tau energy is defined as the energy of the clusters within a 10^0 half opening angle cone around the tau jet direction, which is computed as the sum of the momentum vectors of the calorimetric clusters. In order to separate the hadronic tau candidates from other hadronic jets, the following restrictions are made: not more than 1 track and 5 calorimetric clusters in the region $10^0 < \alpha < 30^0$ are allowed, where α is the half opening angle of a cone around the tau direction and the ratio of the energies deposited in a $10^0 < \alpha < 30^0$ and $0^0 < \alpha < 10^0$ half opening angle cone must be below 0.5.
The leptonically decaying taus are identified as electrons or muons as previously defined.

The low multiplicity event selection

At first, to reject high multiplicity events, less than 10 charged tracks and less than 15 calorimetric clusters in the event are required. To reject the two-photon background the visible energy is required to be larger than $0.2 \cdot \sqrt{s}$. Finally at least three leptons are required in the event if there is a calorimetric deposition in the low polar angle detector, the Active Lead Ring, ALR, and the missing momentum is pointing along the beam axis, i.e. $|\cos\theta| < 0.9$ where θ is the angle between the missing momentum and the beam-axis. Otherwise at least four leptons are required. A minimum energy of 2 GeV for electrons and 3 GeV for muons and taus is required.

In Fig. 2, the comparison between data and Monte Carlo is shown for the energy of all the leptons (excluding those in the low polar angle detector), the invariant mass of the pair of leptons of the same flavour with the highest invariant mass and the corresponding recoiling mass, after all the cuts. In the first plot there are at least three entries per event, depending on the number of selected leptons. The recoiling mass is defined as the missing mass to the choosen pair of leptons. Since there is no unique way to associate leptons coming from the same gauge boson, the ones with the same flavour and the highest invariant mass were choosen, to maximize the probability that they decay from the Z.
The characteristics of the data events which survive the selection at all the three centre-of-mass energies are listed in Table 1.

The high multiplicity event selection

The $\ell\ell q\overline{q}$ events are characterized by hadronic jets and a pair of leptons isolated from the hadronic system. Only the configuration with a pair of isolated electrons or muons is investigated. For $\tau^+\tau^- q\overline{q}$ there is not any dedicated selection, thus the events survived come from the $e^+e^- q\overline{q}$ and $\mu^+\mu^- q\overline{q}$ selections.
To select hadronic events at least 5 charged tracks and 15 calorimetric clusters are required. Moreover the visible energy should be greater than $0.5 \cdot \sqrt{s}$ and finally a pair of electrons or muons, or an electron and a calorimetric deposition in the ALR, is required. The energy of each

lepton is required to exceed 3 GeV. The selected electrons and muons have to satisfy isolation cuts and the tighter set of quality cuts since they are in a hadronic environment.

In Fig. 3, the distributions of the invariant mass of the two selected leptons and their recoiling mass are shown for data and Monte Carlo after all the cuts.
All the data events which survive the selection contain two identified electrons; no events with two muons are selected. The data events which pass the selection at the three centre-of-mass energies are listed in Table 1, where the invariant mass and the recoiling mass of the two electrons are presented.

Systematics

The signal selection efficiency is evaluated using Monte Carlo events. The two main sources of systematic errors are the Monte Carlo statistics and the detector uncertainties and inefficiencies:
a) uncertainty on the energy calibration constants;
b) uncertainty on the global energy scale;
c) tracking inefficiency.
To estimate the effect a), each energy calibration constant was varied independently according to a normal distribution with a standard deviation of 5%, as explained in detail in [11]. To estimate the effect b), the total energy was shifted by $\pm3\%$ and finally, to take into account the effect c), 2% of the tracks were randomly killed in the Monte Carlo events. The net effect of these detector systematics on the signal efficiency is found to be at most 2% which is usually less than the Monte Carlo statistical error.

The dominant error on the background expected events is also due to the the Monte Carlo statistics which gives a contribution at least of $\sim$ 20%. Moreover an overall normalisation error, estimated to be 10%, due to the finite precision of the generators is taken into account.

Results

The efficiencies of the low multiplicity and high multiplicity event selections are reported in Table 2 with the corresponding systematic error from Monte Carlo statistics only. The efficiencies are calculated for events in which all the four fermions have at least an angle of 5^0 with respect to the beam-axis. From the Table 2, it can be noted that the fraction of events $\ell\ell$qq and $\ell\ell'\ell'$ which pass the low and high multiplicity respectively, i.e. the selection not optimized for them, is very small.
The total number of events expected from the signal, the background and the number of events observed in the data after all the cuts are shown in Table 3, where the total error is reported.

Due to the lack of statistics, the cross sections $\sigma_{\ell\ell\ell'\ell'}$ and $\sigma_{\ell\ell\mathrm{qq}}$ of the processes $\ell\ell\ell'\ell'$ and $\ell\ell$qq are determined simultaneously in one variable maximum likelihood fit, fixing the ratio of the two cross sections to the Standard Model value, which corresponds to the determination of the total cross section $\sigma_{\mathrm{tot}} = \sigma_{\ell\ell\ell'\ell'} + \sigma_{\ell\ell\mathrm{qq}}$. The derivation of the cross sections is done independently for the three runs. The total likelihood is given by the product of Poisson probabilities, $P(N_i, \mu_i)$, for the low multiplicity ($i = 1$) and high multiplicity ($i = 2$) selections, having N_i selected events and μ_i expected events:

$$\mu_i = \sum_{j=1,2} \epsilon_{ij}\sigma_j L_i + N_i^{\mathrm{bkgd}},$$

where ϵ_{ij} is the efficiency of selection i to accept events from the process j, where j=1 for the $\ell\ell\ell'\ell'$ channel and j=2 for the $\ell\ell$qq channel. Moreover $N_i^{\rm bkgd}$ is the number of expected events from the background and L_i is the luminosity used in the selection i. Finally σ_j is the cross section for the process j.
Statistical errors corresponding to a 68% confidence level interval are determined by a change of 0.5 in the logarithm of the total likelihood. The systematic error on the cross section is estimated as the RMS of the measured cross section having randomly changed the signal efficiency and the number of expected background events according to their total errors, which is dominated by the Monte Carlo statistics. The resulting total cross section $\sigma_{\rm tot}$ is reported in Table 4 where also $\sigma_{\ell\ell\ell'\ell'}$ and $\sigma_{\ell\ell{\rm qq}}$ are shown. Moreover the Standard Model cross sections, as predicted by EXCALIBUR, are reported. There is agreement between the measured and predicted cross sections.

Acknowledgments

We wish to express our gratitude to the CERN accelerator divisions for the excellent performance of the LEP machine. We acknowledge the contributions of all the engineers and technicians who have participated in the construction and maintenance of this experiment. Those of us who are not from member states thank CERN for its hospitality and help.

References

[1] Physics at LEP2, CERN96-01.

[2] L3 Collab.,A. Adam *et al.*, Phys. Lett. **B 321** (1994) 283.

[3] L3 Collaboration, B.Adeva *et al.*, Nucl.Instr.Meth. **A289** (1990) 35; J.A.Bakken *et al.*, Nucl.Instr.Meth. **A275** (1989) 81; O.Adriani *et al.*, Nucl.Instr.Meth. **A302** (1991) 53; B.Adeva *et al.*, Nucl.Instr.Meth. **A323** (1992) 109; K.Deiters *et al.*, Nucl.Instr.Meth. **A323** (1992) 162; M.Chemarin *et al.*, Nucl.Instr.Meth. **A349** (1994) 345; B.Acciari *et al.*, Nucl.Instr.Meth. **A351** (1994) 300; G. Basti *et al.*, Nucl.Instr.Meth. **A374** (1996) 293; A.Adam *et al.*, Nucl.Instr.Meth. **A383** (1996) 342.

[4] F.A.Berends, R.Kleiss and R.Pittau, Nucl. Phys. **B 424** (1994) 308; Nucl. Phys. **B 426** (1994) 344; Nucl. Phys. (Proc. Suppl.) **B 37** (1994) 163; Phys. Lett. **B 335** (1994) 490; R.Kleiss and R.Pittau, Comp.Phys.Comm. **83** (1994) 14.

[5] J.H.Field, Phys.Lett. **B323** (1994) 432; J.H.Field and T. Riemann, Comp.Phys.Comm. **94** (1996) 53.

[6] S.Jadach, B.F.L.Ward and Z.Was, Comp.Phys.Comm. **79** (1994) 503.

[7] T.Sjöstrand, CERN-TH/7112/93 (1993), revised August 1995; T.Sjöstrand, Comp.Phys.Comm. **82** (1994) 74. T. Sjöstrand, CERN-TH 7112/93 (1993, revised August 1994).

[8] M.Skrzypek *et al.*, Comp.Phys.Comm. **94** (1996) 216; M.Skrzypek *et al.*, Phys.Lett. **B372** (1996) 289.

[9] R.Brun *et al.*, preprint CERN DD/EE/84-1 (Revised 1987).

[10] H.Fesefeldt, RWTH Aachen Report PITHA 85/02 (1985).

[11] L3 Collab.,M. Acciarri *et al.*, Phys.Lett. **B 385** (1996) 454.

Low multiplicity selection			
$\sqrt{s}$ (GeV)	Final State	$M_{\ell\ell}^{\max}$(GeV)	$M_{\rm rec}$(GeV)
130.3	ee$\mu\mu$	85.7 ± 0.8	38.7 ± 3.1
161.3	ee$\mu\mu$	10.1 ± 0.2	108.5 ± 1.6
161.3	ee$\mu\mu$	84.7 ± 2.7	35.3 ± 16.0
172.3	eeee	161.9 ± 1.3	0.0 ± 6.3
172.3	eeee	66.8 ± 0.6	22.5 ± 7.4
High multiplicity selection			
$\sqrt{s}$(GeV)	Final State	$M_{\ell\ell}$(GeV)	$M_{\rm rec}$(GeV)
136.3	eeqq	81 ± 10	49 ± 5
161.3	eeqq	78.1 ± 0.7	38.5 ± 4.1
172.3	eeqq	76.2 ± 0.7	38.6 ± 4.5
172.3	eeqq	145.1 ± 1.2	11.3 ± 24.3

Table 1: Candidates of the low multiplicity selection: the di-lepton invariant mass ($M_{\ell\ell}^{\max}$(GeV)) and the corresponding recoiling mass ($M_{\rm rec}$(GeV)) of the same flavoured lepton pair with the biggest invariant mass are reported. Candidates of the high multiplicity selection: the invariant mass of the di-lepton pair ($M_{\ell\ell}$(GeV)) and their recoiling mass ($M_{\rm rec}$(GeV)) are reported.

Signal efficiencies			
Selection	$\sqrt{s}$	$\ell\ell\ell\ell$ Channel	$\ell\ell$qq Channel
Low Multiplicity	$130 - 136$ GeV	$(8.1 \pm 0.3)\%$	$(0.06 \pm 0.02)\%$
	161 GeV	$(6.8 \pm 0.2)\%$	$(0.05 \pm 0.01)\%$
	$170 - 172$ GeV	$(7.7 \pm 0.2)\%$	$(0.08 \pm 0.02)\%$
High Multiplicity	$130 - 136$ GeV	$(0.32 \pm 0.06)\%$	$(8.5 \pm 0.6)\%$
	161 GeV	$(0.27 \pm 0.03)\%$	$(7.1 \pm 0.2)\%$
	$170 - 172$ GeV	$(0.25 \pm 0.03)\%$	$(7.7 \pm 0.2)\%$

Table 2: Low multiplicity and high multiplicity event selection efficiencies for the $\ell\ell\ell'\ell'$ and $\ell\ell$qq channels with the corresponding Monte Carlo statistics error.

Process	$\sqrt{s} = 130 - 136$ GeV	$\sqrt{s} = 161$ GeV	$\sqrt{s} = 170 - 172$ GeV
eeee	0.50 ± 0.02	0.66 ± 0.04	0.65 ± 0.04
$ee\mu\mu$	0.29 ± 0.02	0.38 ± 0.06	0.35 ± 0.05
$ee\tau\tau$	0.10 ± 0.01	0.14 ± 0.03	0.13 ± 0.03
$\mu\mu\mu\mu$	0.0250 ± 0.0008	0.029 ± 0.002	0.024 ± 0.002
$\mu\mu\tau\tau$	0.024 ± 0.001	0.029 ± 0.003	0.025 ± 0.002
$\tau\tau\tau\tau$	0.0034 ± 0.0004	0.0051 ± 0.0009	0.0034 ± 0.0006
$\ell\ell\ell'\ell'$	0.95 ± 0.03	1.23 ± 0.08	1.18 ± 0.07
eeqq	0.93 ± 0.03	1.16 ± 0.06	1.09 ± 0.06
$\mu\mu$qq	0.210 ± 0.004	0.27 ± 0.01	0.29 ± 0.01
$\tau\tau$qq	0.012 ± 0.001	0.014 ± 0.002	0.012 ± 0.002
$\ell\ell$qq	1.15 ± 0.03	1.45 ± 0.06	1.40 ± 0.06
Total	2.10 ± 0.05	2.7 ± 0.1	2.6 ± 0.1
Bkgd	0.8 ± 0.3	0.8 ± 0.09	0.8 ± 0.2
Data	2	3	4

Table 3: Number of four-fermion and background expected events and data observed with their systematic errors.

Cross Sections (pb)			
	$\sqrt{s} = 130 - 136$ GeV	$\sqrt{s} = 161$ GeV	$\sqrt{s} = 170 - 172$ GeV
σ_{tot}	$2.9^{+4.2}_{-2.6} \pm 0.2$ (5.2)	$3.3^{+2.7}_{-1.8} \pm 0.06$ (3.4)	$4.1^{+3.0}_{-2.1} \pm 0.08$ (3.2)
$\sigma_{\ell\ell\ell'\ell'}$	$1.4^{+2.0}_{-1.2} \pm 0.08$ (2.5)	$1.5^{+1.3}_{-0.8} \pm 0.03$ (1.6)	$1.8^{+1.3}_{-1.0} \pm 0.04$ (1.4)
$\sigma_{\ell\ell\text{qq}}$	$1.5^{+2.2}_{-1.3} \pm 0.09$ (2.7)	$1.8^{+1.5}_{-1.0} \pm 0.03$ (1.9)	$2.2^{+1.6}_{-1.2} \pm 0.04$ (1.7)

Table 4: Measured total cross section σ_{tot} for the final states $\ell\ell\ell'\ell'$ and $\ell\ell$qq. The cross section values ($\sigma_{\ell\ell\ell'\ell'}$, $\sigma_{\ell\ell\text{qq}}$) for the two processes are also reported having fixed the ratio of them to the Standard Model value. The first uncertainty for the cross sections is the statistical error, the second is the systematical one. In brackets the Standard Model values of the cross sections, as predicted by EXCALIBUR, are reported.

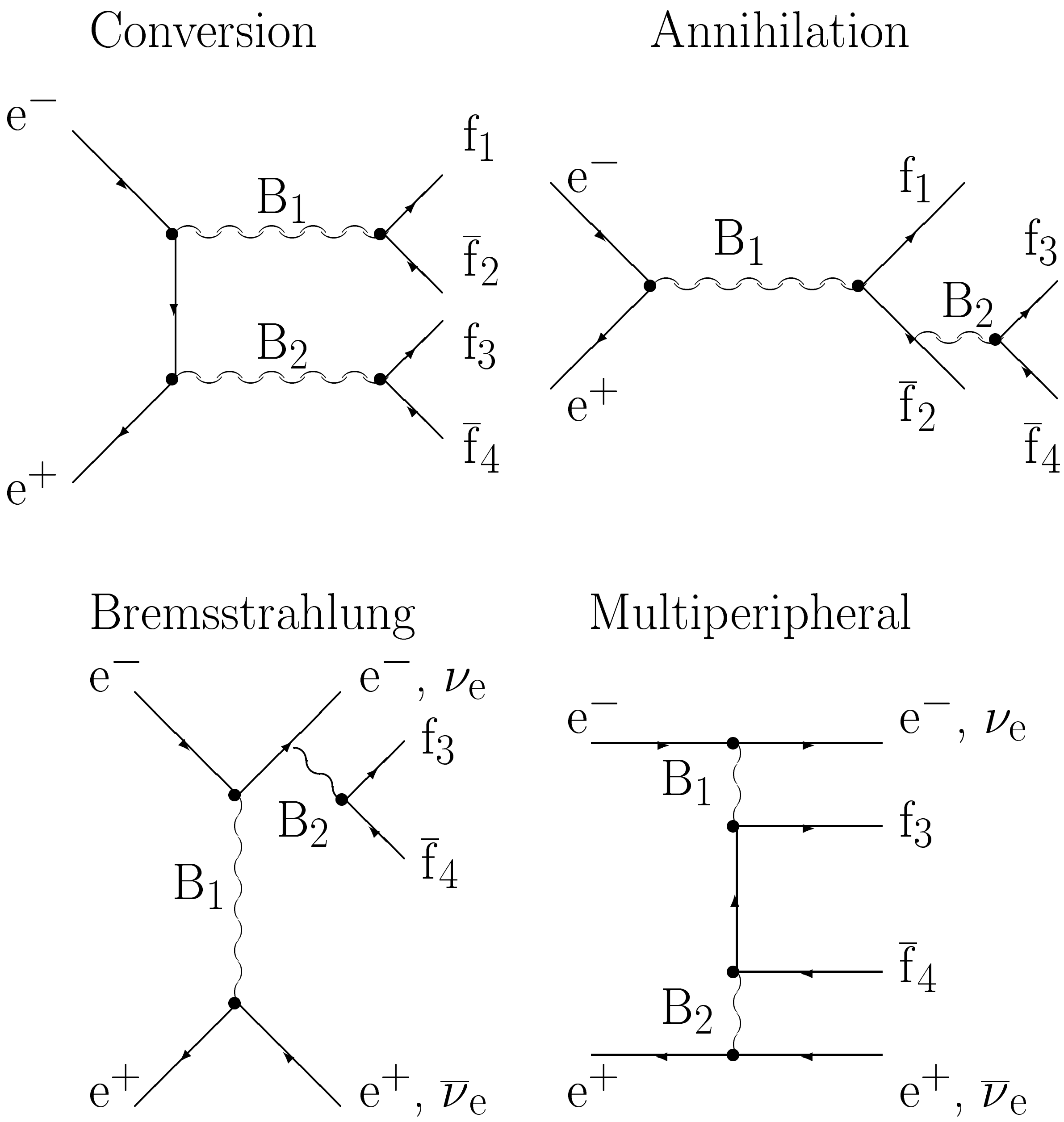

Figure 1: Topologies of the lowest order Feynman diagrams for the $e^+e^- \to f_1\bar{f}_2f_3\bar{f}_4$ process, neutral gauge current mediated (B_1,B_2=γ, Z).

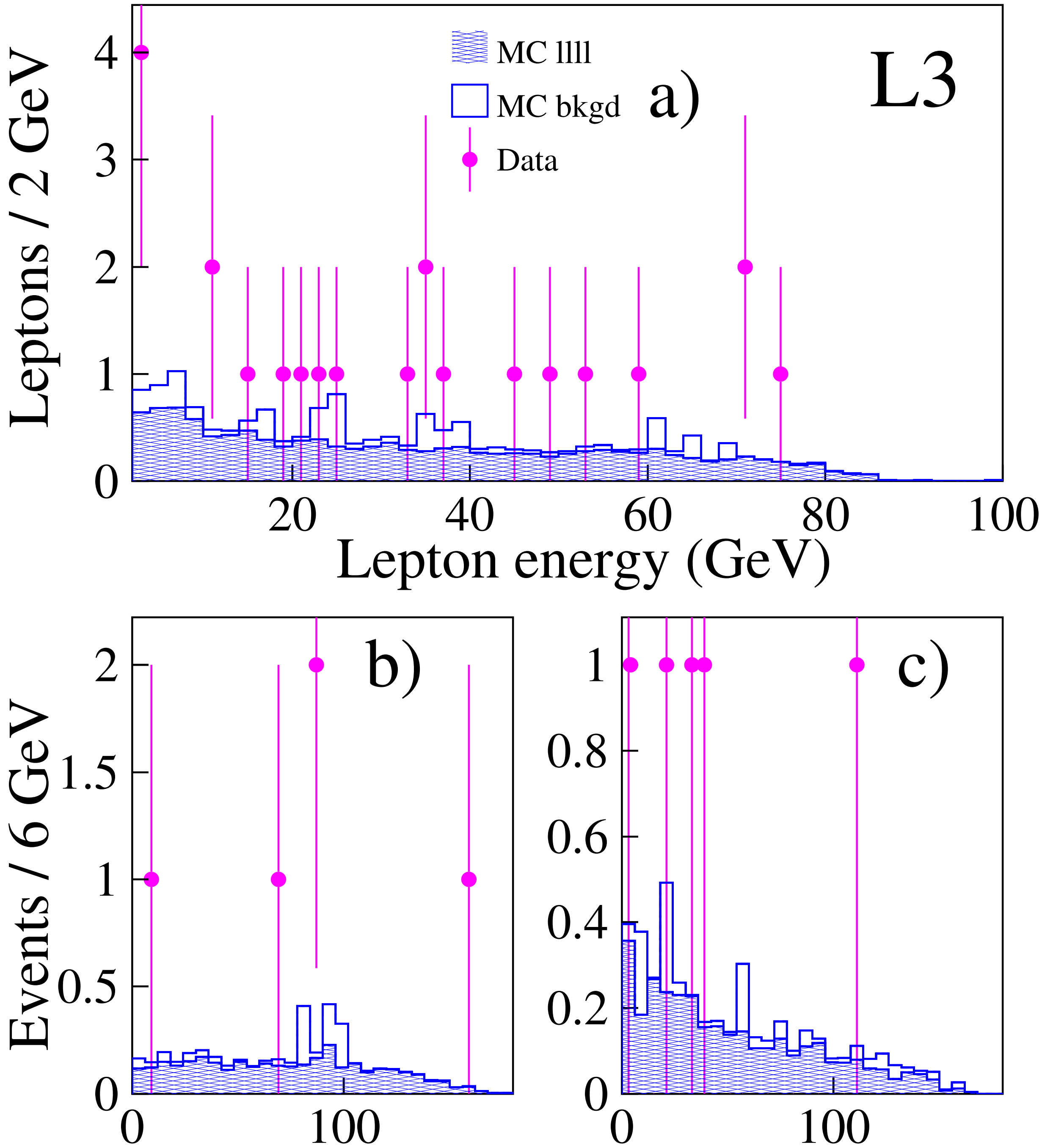

Figure 2: Energy of the leptons (a), highest invariant mass of a pair of identified leptons of the same flavour (b) and their recoiling mass (c) for the low multiplicity selection. The histograms are the expected distributions for the four-fermion events, summed to the background events, compared to the data distributions, shown by the dots.

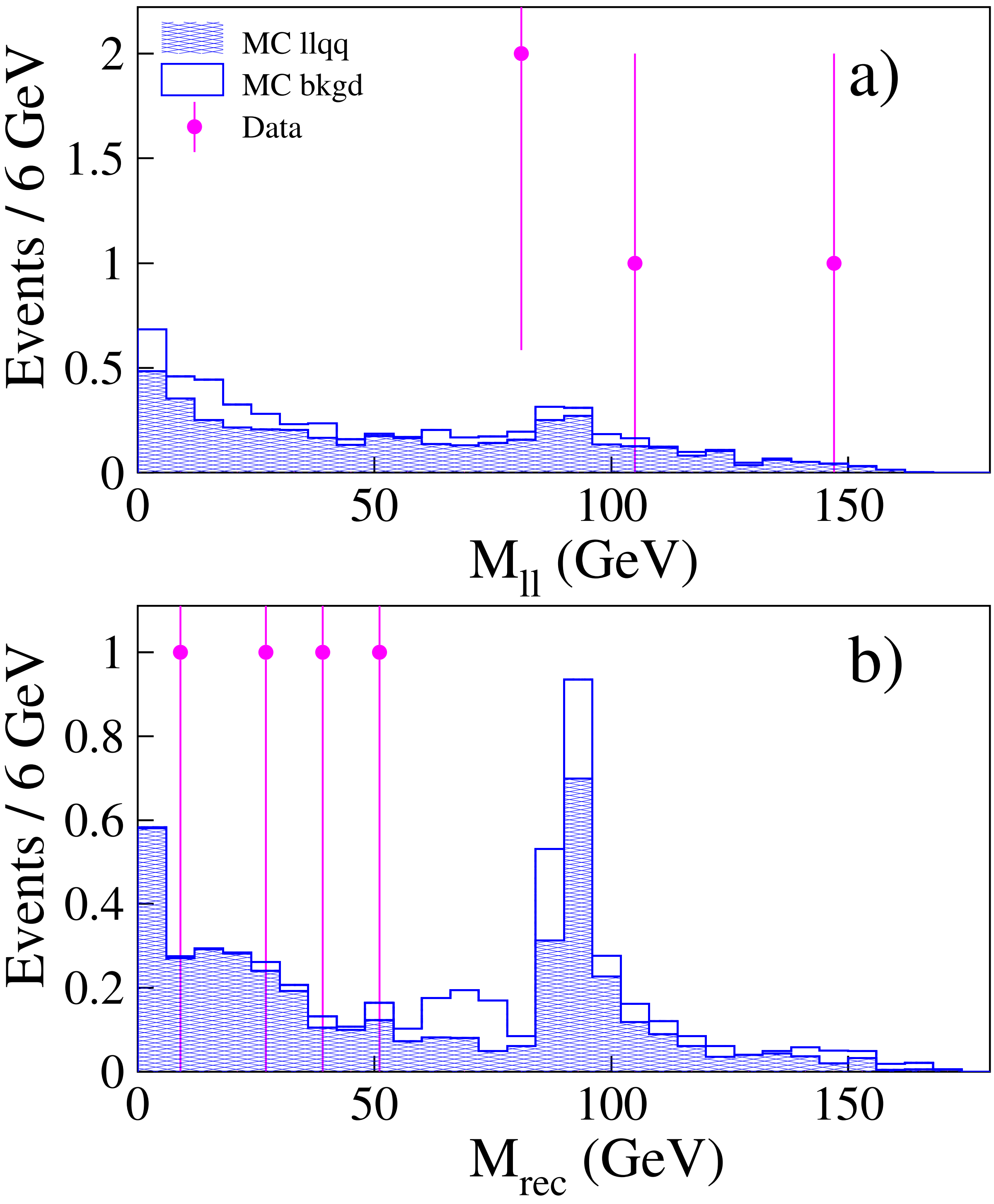

Figure 3: Invariant mass of the pair of identified electrons or muons (a), and their recoiling mass (b) for the high multiplicity selection. The histograms are the expected distributions for the four-fermion events, summed to the background distributions. Data events are shown by the dots.